



# Changes in the Phenolic Fraction of Protobind 1000 and Bacterial Microbiota in the Gut of a Higher Termite, *Nasutitermes ephratae*

Jusselme MD<sup>1</sup>, Cézard L<sup>2</sup>, Pion F<sup>2</sup>, Baumberger S<sup>2</sup>, Robert A<sup>1</sup>, Lapierre C<sup>2</sup>,  
Diouf M<sup>1</sup>, Mora P<sup>1</sup> and Miambi E<sup>1\*</sup>

<sup>1</sup>Institut d'Ecologie et des Sciences de l'Environnement de Paris (iEES Paris), Université Paris Est Créteil, France

<sup>2</sup>Institut Jean-Pierre Bourgin, France

## Research Article

Volume 5 Issue 3

Received Date: August 17, 2020

Published Date: September 22, 2020

DOI: 10.23880/oajmb-16000169

**\*Corresponding author:** Dr Edouard Miambi, Associate Professor, University Paris Est Créteil

/IEES-Paris, 61 Avenue du Général de Gaulle 94010 Créteil Cedex France, France, Tel: + 33145171507; Email: miambi@u-pec.fr

## Abstract

Termites are examples of natural biomass utilization systems that have evolved to overcome the recalcitrance of lignin to degradation. To investigate the application of this to the conversion of technical lignins produced by biorefineries, a higher wood-feeding termite species, *Nasutitermes ephratae*, was fed with a commercial grass soda lignin (Protobind 1000, PB1000). We investigated the fate of PB1000 in termite guts and the changes in gut microbiota that occurred using Pyrolysis - Gas Chromatography / Mass Spectrometry (Py-GC/MS) and high-throughput sequencing of the 16S rRNA genes. The worker caste termites fed with PB1000 had only half the survival rate of the controls and increased the PB1000 syringyl/guaiacyl ratio from 1.74 to 2.26. The changes in the syringyl/guaiacyl ratio were consistent with the degradation of the free phenolic monomers in PB1000 inside the termite gut, and they were associated with the increase in the relative abundance of Firmicutes and Bacteroidetes. This work showed the ability of the digestive tract of a wood-feeding higher termite species, *N. ephratae*, to metabolize the free-volatile phenolic monomers in PB1000. Overall, our results identified bacterial candidates for the development of a bacterial inoculum in pretreatment processes for the utilization of technical lignin in biorefineries.

**Keywords:** Technical Lignin; Protobind 1000; Grass Soda Lignin; Natural Biomass Utilization Systems; Gut Bacterial Community; Higher Termite; Py-GC/MS; Biorefinery

**Abbreviations:** PB1000: Protobind 1000; KL: Klason Lignin; IRD: Institute of Research For Development; OTU: Operational Taxonomic Unit; NGS: Next-Generation Sequencing; ; Py-GC/MS: Pyrolysis Gas Chromatography Mass Spectrometry

## Introduction

The recalcitrance of lignins in pretreatment processes is an obstacle to the efficient utilization of lignocellulosic biomass for biofuel production and value-added biochemicals

[1,2]. Consequently, over the past decades, studies have been directed towards Natural Biomass Utilization Systems (NBUS), natural systems that can efficiently degrade and utilize lignocellulosic biomass [3]. Termites consume 3-7 billion tons of lignocellulosic materials annually [4] and thereby represent one of the most prolific and efficient NBUS. With their microbial symbionts, which mostly consist of specific lineages that have co-evolved or converged with their specific host [5], termites have developed efficient mechanisms for biomass utilization. These microbial communities are very dense (up to 10<sup>11</sup> cells/mL), diverse

(6,000 phylotypes/mL or 740 phylotypes by gut), with many lineages of mostly uncultivated bacteria that exclusively occur in this habitat [6]. Many putative cellulases, xylanases, and other glycoside hydrolases, associated with the bacterial symbiont groups and involved in lignocellulose degradation, have been found in termite guts [7]. Lignocellulose digestion in termites is a mutualistic system combining the activities of both the hosts and their bacterial symbionts [8]. Extensive work has been devoted to study lignocellulose degradation by wood-feeding lower termite species. Lower termites harbor symbiotic flagellate protozoa that are known to be sources of cellulases and hemicellulases. Evidence has been brought of the abilities of termite digestive systems and their associated gut bacteria to metabolize aromatic compounds and dimeric lignin model compounds [9-11]. Furthermore, most previous studies devoted to the *in-vivo* degradation of aromatic polymeric lignins by insects have also focused on lower wood-feeding termites. In these studies, modifications of the lignin in the digestive tract varied from weak [12,13] to more pronounced [14-17]. These discrepancies may be accounted for by the structural variability of the lignins used in these studies (depending on their botanical origin and/or their isolation procedure) and by the analytical tools used.

Fewer studies have been devoted to lignin degradation by higher termites, which harbor exclusively prokaryotic symbionts and have a diverse diet [18,19]. The loss of flagellates in higher termites suggests that new functions have been gained by the prokaryotic microorganisms in the digestive process [19]. Many lignin-degrading candidates have been reported, but single strains show limited lignin utilization ability [20]. With the emerging role for bacteria in lignin degradation [21,22], the exploration of the greater bacterial biodiversity in higher termite guts for bacterial catalytic systems could provide a route to the development of an inoculum for pretreatment processes for the efficient utilization of technical lignins.

The present study investigates, for the first time, whether a technical grass soda lignin, Protobind 1000 (PB1000) can be metabolized by the gut microbiota of a higher termite species. We posed the hypothesis that the strong axial dynamics of oxygen status and redox potential, together with the continuous influx of oxygen across the gut wall [23], create aerobic or microaerobic conditions in the gut of higher termites. This environment may be especially attractive as canonical lignin degradation involves peroxide- or oxygen-dependent enzymes [24]. A higher wood-feeding termite species, *N. ephratae* was fed with PB1000 to test this hypothesis. The effects of PB1000 on the physiological activities of *N. ephratae* were investigated by monitoring (i) the survival rates of the termites as compared to controls fed on the usual birch wood diet, (ii) the changes in the gut bacterial community (iii) and the modifications of the

chemical structure of this technical lignin. A high-throughput, second-generation sequencing approach was used to assess the changes in termite-gut bacterial microbiota [25,26]. Analytical pyrolysis, combined with gas chromatography/mass spectrometry (Py-GC/MS), was selected to compare the chemical structure of the undigested PB1000 with digested samples in the termite gut, as it is widely used to investigate the chemical structure of lignins and biomass [27,28].

## Material and Methods

### Technical Lignin Source and Composition

A commercial grass soda lignin, PB1000 (Green Value Entreprises LLC, USA), isolated from mixed wheat straw and sarkanda bagasse, was used for the termite feeding experiments. Lignin was determined as Klason lignin (KL) by gravimetric analysis with a two-step sulfuric acid hydrolysis of the sample (300 mg) and correction for ash content, as described previously [29]. Neutral sugars were analyzed by sequential two-step acidic hydrolysis of the sample (10 mg) using aqueous trifluoroacetic acid (TFA, 2.3 M, 2 h, 110°C), then sulfuric acid (51% w/w H<sub>2</sub>SO<sub>4</sub>, 1 h, ambient temperature, then 5% w/w H<sub>2</sub>SO<sub>4</sub>, 2 h, 100°C). The neutral monosaccharides recovered by TFA and H<sub>2</sub>SO<sub>4</sub> hydrolysis were assigned to hemicellulose-derived sugars and cellulose-derived glucose, determined by high-performance anion-exchange chromatography with amperometric detection using fucose as an internal standard as previously described by Sipponen et al. [30].

Free phenolics were extracted from 10 mg samples with 0.025 mg *o*-coumaric acid (internal standard) in 1 mL water with 0.1% (v/v) HCOOH. The phenolics were extracted for 2 h at room temperature with constant agitation at 350 rpm. The mixture was then centrifuged at 2,000 x g for 10 min at room temperature. The supernatant was then purified using a Sep-Pack tC18 cartridge (Waters, Guyancourt, France) and analyzed by HPLC-UV, as previously described by Lapierre et al. [31]. All the analyses were performed in duplicate (error < 3%). The composition is expressed in mg/g.

### Termite Collection and Feeding Experiment

Higher wood-feeding termites, *N. ephratae*, were obtained from a laboratory colony at IEES, Bondy (IRD, Institute of Research for Development – France Nord). The colony was maintained in a termite rearing room on a 12-h light/dark cycle at 27°C ± 2°C, 80% relative humidity, and fed with birch wood. Worker caste termites were used for the experiment. The experimental method was based on our previous studies of termite behavior and our experience of handling them. We used two sets of triplicate crystal polystyrene lab boxes (60 × 43 × 50 mm, W × L × H, Thermo Fisher Scientific, France)

containing 20 g of sterile Fontainebleau sand mixed with either 0.25 g powdered PB1000 or 0.25 g birch sawdust (controls). Two hundred termites were added to each box. About 0.5 mL of sterile distilled water was added every three days to each box to humidify the sand. The number of live workers was recorded every day for six days. At the end of the experiment, the termite guts were isolated using fine, sterile forceps, placed into 2-mL Eppendorf tubes and immediately frozen at  $-20^{\circ}\text{C}$  for DNA extraction or frozen at  $-20^{\circ}\text{C}$  and freeze-dried for Py-GC/MS analysis.

### DNA Extraction, Amplification, Sequencing and Sequence Processing

Twenty-five termite-guts were first crushed using a polypropylene micro pestle in 1.5 mL microtubes containing 1 mL of Ringer solution [32] and centrifuged at  $11,000 \times g$  for 15 min at  $4^{\circ}\text{C}$ . The pellets were suspended in NucleoSpin Soil Solution C1 buffer. Then the DNA was extracted using the NucleoSpin Soil isolation kit (Macherey-Nagel, Germany) following the manufacturer's instructions. DNA extracts from the triplicates were pooled, and the concentrations were quantified using an ND-1000 Spectrophotometer (Nano Drop products, Wilmington, USA). Aliquots of the DNA solutions adjusted to the same concentration were sent to the Research and Testing Laboratory (Lubbock, TX, USA) for amplification and sequencing. The V1-V2 variable regions of the 16S rRNA genes were amplified using the bacterial primers 28F and 338R and sequenced using  $2 \times 250$  paired-end Illumina MiSeq platform. The raw sequence data have been deposited in the NCBI Sequence Read Archive under the BioProject PRJNA550212.

The data were demultiplexed, and pair-end reads were joined by the GeT platform, using Flash v1.2.6 [33], and the barcode and primer sequences were removed with cutadapt [34]. Subsequently, the sequences were aligned to the SILVA reference database release 128 [35] and preclustered (pre-cluster,  $\text{diffs}=1$ ). Chimeras were removed using VSEARCH [36]. Amplicon sequences (12,559) were randomly subsampled from the dataset to account for differences in sampling effort. Sequences were then clustered into operational taxonomic units (OTU) with SWARM [37], which generates the OTU abundance table with an OTU being defined at the 97% sequence similarity level. The taxonomic affiliation for each OTU was determined using DictDb v3, the reference database dedicated to insect-associated bacteria [38].

### Py-GC/MS Analyses

The initial birch wood sawdust and PB1000 samples, as well as the freeze-dried guts of termites fed with either birch or PB1000 samples, were analyzed using Py-GC/MS

as recently described by Voxeur et al. [39]. Analyses were carried out using a CDS model 5250 pyroprobe autosampler interfaced to an Agilent 6890/5973 GC/MS. The samples (400  $\mu\text{g}$ ) were pyrolyzed in a quartz tube at  $500^{\circ}\text{C}$  for 15 s. The volatile pyrolysis products were separated on GC capillary column (5% phenyl methyl siloxane, 30 m, 250  $\mu\text{m}$  i.d., and 0.25  $\mu\text{m}$  film thickness) using helium as the carrier gas with a flow rate of 1 mL/min. The pyrolysis and GC/MS interfaces were kept at  $290^{\circ}\text{C}$  and the GC was temperature-programmed from  $40^{\circ}\text{C}$  (1 min) to  $130^{\circ}\text{C}$  at  $+6^{\circ}\text{C min}^{-1}$ , then from 130 to  $250^{\circ}\text{C}$  at  $+12^{\circ}\text{C min}^{-1}$  and finally from  $250^{\circ}\text{C}$  to  $300^{\circ}\text{C}$  at  $+30^{\circ}\text{C min}^{-1}$  (3 min at  $300^{\circ}\text{C}$ ). The MS was operated in the electron impact mode (70 eV) for  $m/z$  from 40 to 450. The various phenolic pyrolysis compounds were identified by comparison with the spectra of authentic compounds or published spectra [40]. The peak areas of the main pyrolysis-derived phenolics were identified and evaluated using the Automatic Mass Spectral Deconvolution and Identification System (AMDIS version 2.69).

In addition to the one-step pyrolysis method performed as described above, the initial PB1000 sample was analyzed using a two-step thermal treatment. The first treatment at  $200^{\circ}\text{C}$  for 20 s was performed to simply volatilize low molecular weight aromatics, if any, followed by the pyrolysis step at  $500^{\circ}\text{C}$  for 15 s, to degrade the non-volatile compounds into a mixture of volatile pyrolysis adducts.

### Statistical Analysis

Before the various analyses were performed to test for significant differences between the treatments, the normality of the data matrices was tested using the Kolmogorov Smirnov test implemented in R-3.6.1 software (France). Differences between the termite survival rates and the digested and undigested substrates were analyzed by one-way ANOVA (Fisher's Post Hoc Test) with a 95% confidence interval.

## Results

### Chemical Composition of PB1000 and its Effect on Survival Rates of Termites

KL was the principal constituent of the PB1000 sample (Table 1). Neutral sugars accounted for 1.9% and were mainly xylose (67% of total carbohydrates). Monomeric phenolics accounted for about 1.4%, primarily acetosyringone, syringaldehyde, vanillin, *p*-coumaric acid, and ferulic acid in decreasing order of abundance. Figure 1 show the survival rates of termites fed on PB1000 and the controls fed on birch sawdust. The survival rates of the PB1000-fed termites and the controls were similar on the first day of the experiment. From the second day, the survival rates were lower for

PB1000-fed termites than for the controls. The differences in survival rates were statistically significant ( $P < 0.05$ , Fischer's

PLSD-test) from the second day until the end of experiments (6 days).

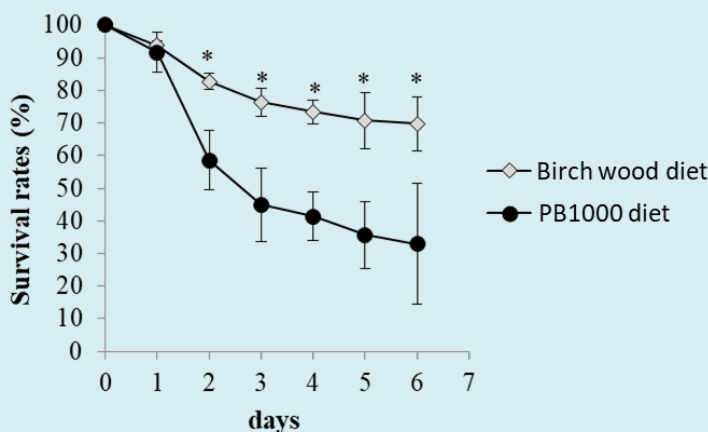


**Figure 1:** Effect of diet on the survival rate of the termites. The differences between the PB1000-fed termites and the controls were significant from day 2 (\* $p < 0.05$ , Fischer's PLSD post-doc test).

Component	Amount (mg/g)
Klason lignin <sup>a</sup>	881.1 (4.6)
Total carbohydrates <sup>b</sup>	18.51 (0.83)
including	
xylose	12.31 (0.14)
arabinose	2.67 (0.02)
glucose	2.14 (0.49)
galactose	1.39 (0.21)
Total phenolic monomers	13.7 (4.6)
including	
acetosyringone	4.76 (0.08)
syringaldehyde	2.27 (0.04)
vanillin	1.99 (0.04)
<i>p</i> -Coumaric acid	1.13 (0.01)
ferulic acid	1.09 (0.03)
Ash	14.4 (1.99)

**Table 1:** Composition of the PB1000 sample.

Data are mean values ( $n=3$ ) with the standard deviations in parentheses.

<sup>a</sup> Acid-insoluble lignin corrected for ash content after two-step acid hydrolysis.

<sup>b</sup> Neutral monosaccharides determined after TFA hydrolysis (no cellulose-derived glucose was detected after  $H_2SO_4$  hydrolysis).

### Changes in the Structure of the Gut Bacterial Microbiota of *N. Ephratae* Workers Fed with PB1000

The gut bacterial microbiota of the worker caste termites directly after collection from the nest was dominated by the Spirochaetes (67%), followed by Fibrobacteres (18%) (Figure 2). The relative abundance of the Spirochaetes decreased when the termites were fed with either PB1000 or birch wood, although this decrease was higher for the PB1000-fed termites than for the controls. For the PB1000-fed termites, there was also a dramatic reduction in the relative abundance of Fibrobacteres with a corresponding increase in the relative abundances of Bacteroidetes and Firmicutes. For the controls, there were no noticeable changes in the structure of the bacterial community between 3 and 6 days. In particular, the relative abundance of Fibrobacteres was similar to that for termites collected directly from the nest. Spirochaetes were mainly represented by phylotypes assigned to *Spirochaetaceae\_Treponema* across all samples (Figure 3). Feeding termites with PB1000 drastically reduced the relative abundance of bacteria assigned to Termite\_cluster\_I (Fibrobacteres) and, to a lesser extent, those assigned to *Rhodospirillaceae* (Proteobacteria) while increasing the relative abundance those assigned to *Porphyromonadaceae\_3*, *Porphyromonadaceae\_Gut\_group*, *Rikenellaceae* (Bacteroidetes); *Desulfovibrionaceae* (Proteobacteria); Insect\_cluster, *Family\_XIII\_Incertae\_Sedis*, *Ruminococcaceae*, and *Peptococcaceae\_1* (Firmicutes).

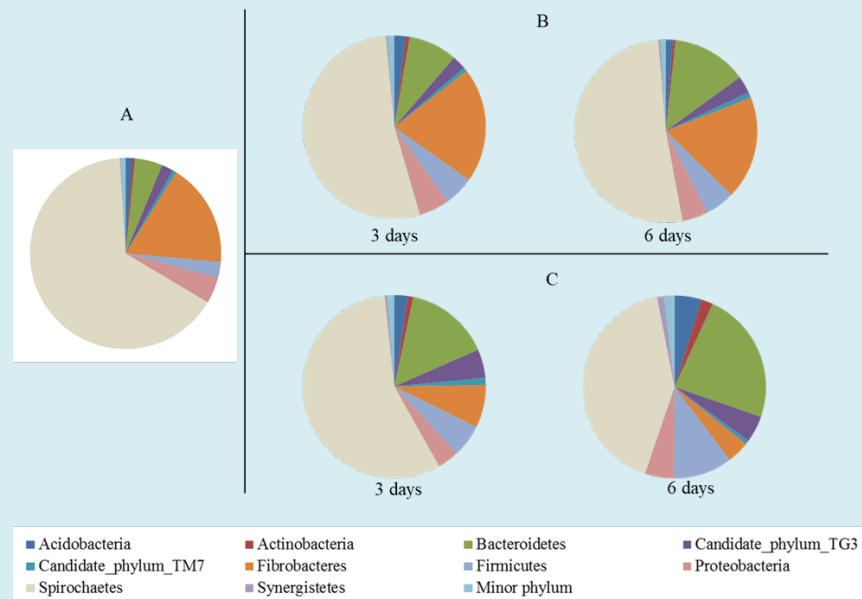


**Figure 2:** Changes in the relative abundance of the major phyla in the termite guts: A) directly collected from their nest, B) fed with birch and C) fed with PB1000.

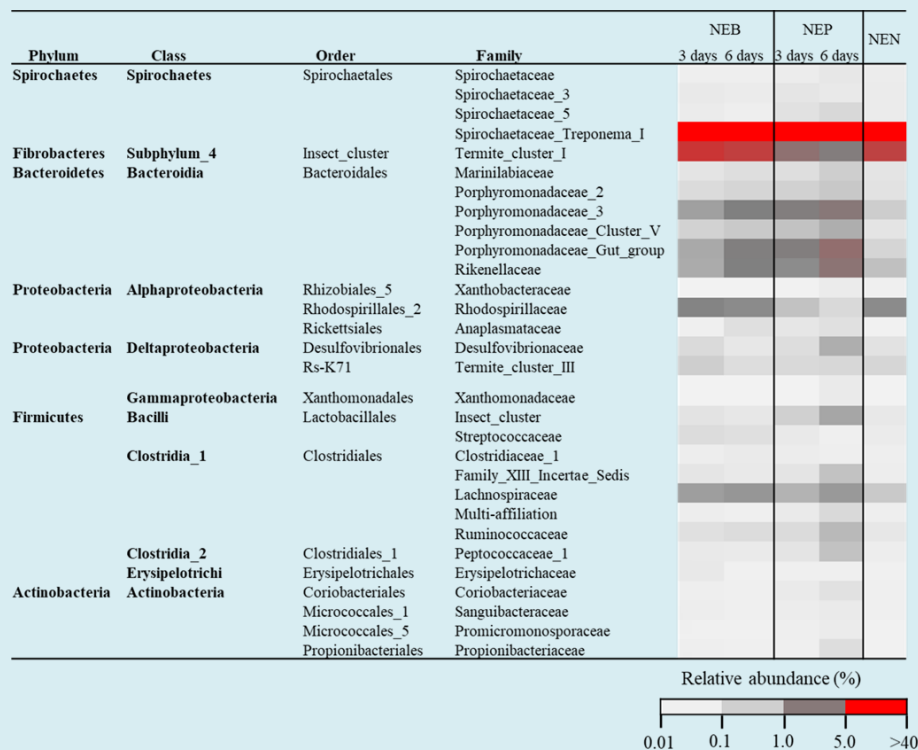


**Figure 3:** Heatmap of the relative abundance of the major bacterial taxa in the guts of termites fed with birch wood (NEB), fed with PB1000 (NEP), and directly collected from their nest (NEN). Classification is shown down to the family level.

### Py-GC/MS analyses of PB1000 and birch wood before and after digestion in the gut of *N. ephratae*

Figure 4 shows the Py-GC/MS pyrograms of the major volatile compounds for the initial PB1000 and birch wood samples and treatments applied. The main phenolics identified were representatives of guaiacyl (G) compounds (peaks 3, 4, 6, 7, 9, 11, 12, and 14) and syringyl (S) compounds (peaks 8, 10, 13, 15, 16, 17, 18 and 19). Vinylphenol (peak 5) was found only in the pyrograms from PB1000-fed

termites. The total G compounds were calculated excluding vinylguaiacol (peak 7) as this product may originate from G lignin units as well as from ferulate units that occur in grass samples [34]. The pyrograms for the guts of both PB1000-fed termites and the controls (Figures 4B and 4D) show peaks (P1, P2, P3) that are not visible for the initial PB1000 and birch samples. These could be assigned to protein-derived pyrolysis products. The relative abundances of the main phenolics released by the pyrolysis of PB1000 and birch wood, before and after digestion by *N. ephratae* gut are given in Table 2.

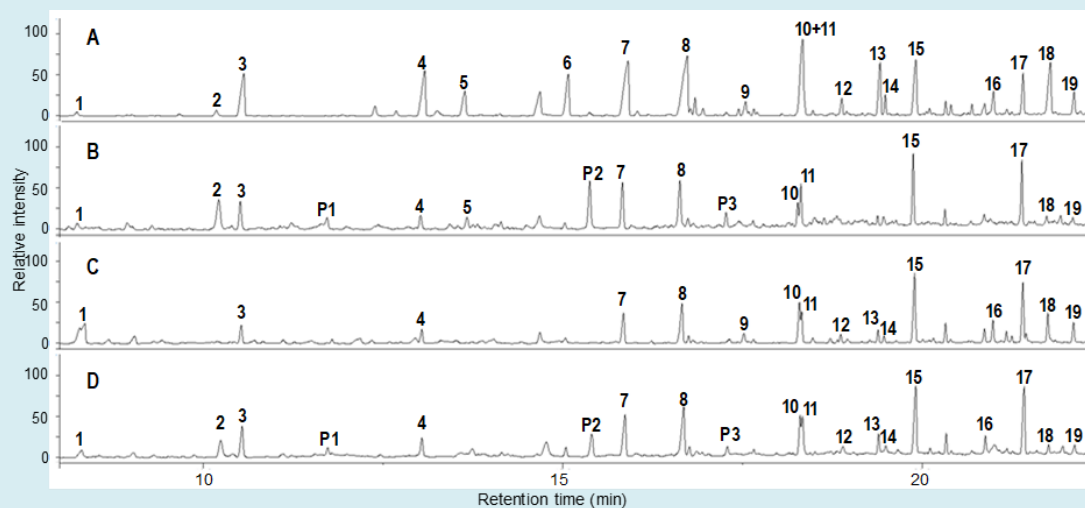


**Figure 4:** Partial pyrograms (total ion chromatograms) of A) Initial PB1000 sample, B) termite guts containing digested PB1000, C) birch wood sample, and D) termite guts containing digested birch wood.

Peak numbers correspond to the following compounds. 1: 4-hydroxy-5,6-dihydropyran-2-one; 2: 4-methylphenol; 3: guaiacol; 4: 4-methylguaiacol; 5: 4-vinylphenol; 6: 4-ethylguaiacol; 7: 4-vinylguaiacol; 8: syringol; 9: vanillin; 10: 4-methylsyringol; 11: 4-allylguaiacol; 12: acetoguaiacol; 13: 4-ethylsyringol; 14: guaiacylacetone; 15: 4-vinylsyringol; 16: syringaldehyde; 17: 4-allylsyringol; 18: acetosyringone; 19: syringylacetone. P1, P2, and P3 are peaks specific to termite gut samples and indicate proteins corresponding to phenylacetone nitrile (P1), indole (P2), and methylindole (P3). Peak 2 could also originate from protein tyrosine residues.

Pyrolysis compounds (peak numbers shown in Figure 4)	Birchwood		PB1000	
	Initial sample	In termite guts	Initial sample	In termite guts
Vinylphenol (VP) (peak 5)	Traces	Traces	3.97 (0.17)b	3.35 (0.18)a
Vinylguaiacol (VG) (Peak 7)	8.97 (0.50)a	13.31 (0.26)b	13.68 (0.85)b	13.25 (1.61)b
G compounds (sum of peaks 3, 4, 6, 9, 11, 12, 14)	22.68 (1.24)a	25.22 (0.76)b	30.08 (0.22)c	25.61 (0.28)b
S compounds (sum of peaks 8, 10, 13, 15 to 19)	68.34 (1.66)d	61.48 (0.87)c	52.28 (1.12)a	57.80 (2.07)b
S/G ratio	3.03 (0.23)c	2.44 (0.11)b	1.74 (0.05)a	2.26 (0.10)b
Vanillin (peak 9)	2.35 (0.14)b	Traces	1.42 (0.03)a	Traces
Syringaldehyde (peak 16)	4.38 (0.32)b	Traces	2.19 (0.08)a	Traces
Acetosyringone (peak 18)	3.86 (0.48)b	1.72 (0.06)a	7.15 (0.30)c	1.81 (0.07)a

**Table 2:** Relative abundance of the major low molecular weight phenolics released by pyrolysis of PB1000 and birch wood before and after a 6-day digestion in *N. ephratae* gut (expressed in % of the total area). S: syringyl-type phenolic compounds; G: guaiacyl-type phenolic compounds.

Data are mean values ( $n=3$ ) with the standard deviations in parentheses. Differences were tested using ANOVA and Fisher's PLSD post-hoc tests and values followed by different letters are significantly different ( $P < 0.05$ ).

Digestion by the termites increased the pyrolysis S/G ratio of PB1000 and decreased the S/G ratio of birch wood. The results were significantly different ( $P < 0.05$ , Fisher's PLSD post-hoc tests). Digestion reduced the relative abundances of vanillin (G-CHO, peak 9), syringaldehyde (S-CHO, peak 16), and acetosyringone (S-CO-CH<sub>3</sub>, peak 18) for both PB1000 and birch wood ( $P < 0.05$ , Fisher's PLSD

post-hoc tests). As acetosyringone, syringaldehyde, and vanillin were the main low molecular weight phenolics in the PB1000 sample (Table 1). The source of these free phenolics to the pyrolysis trace was evaluated by subjecting PB1000 to an initial thermal treatment at 200°C, followed by the pyrolysis step at 500°C. This aimed at volatilizing low molecular weight compounds and showed that these phenolics in the pyrogram for the initial PB1000 sample partially originate from free acetosyringone, syringaldehyde, and vanillin. These compounds were almost absent from the pyrogram for the PB1000-fed termite guts (See additional file Figure 5).

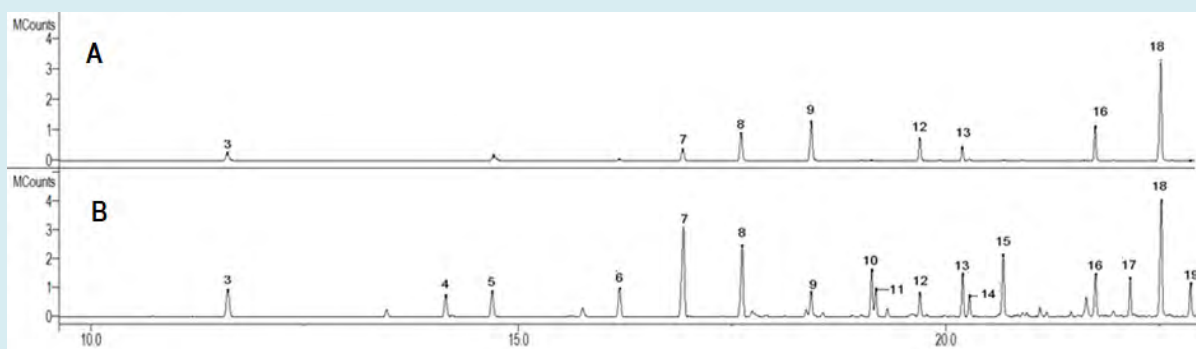


**Figure 5:** GC/MS analyses (total ion chromatograms) of the low molecular weight phenolics released by two successive thermal treatments of PB1000 sample A) 200°C (with simple volatilization of soluble phenolics) and B) 500°C (genuine pyrolysis). Peak numbers correspond to the following compounds. 3: guaiacol; 4: 4-methylguaiacol; 5: 4-vinylphenol; 6: 4-ethylguaiacol; 7: 4-vinylguaiacol; 8: syringol; 9: vanillin; 10: 4-methylsyringol; 11: 4-allylguaiacol; 12: acetoguaiacone; 13: 4-ethylsyringol; 14: guaiacylacetone; 15: 4-vinylsyringol; 16: syringaldehyde; 17: 4-allylsyringol; 18: acetosyringone; 19: syringylacetone.

## Discussion

There is still little information in the literature on the ability of bacterial gut microbiota of higher termites to degrade technical lignin since most studies have focused on lower termites and natural lignins. This is the first study of the fate of a technical grass soda lignin, PB1000, in the digestive system of a higher wood-feeding termite species, *N. ephratae*. It also describes the effect of the ingestion of PB1000 on survival rates and the structure of the gut microbiota community. The substrate PB1000 was selected for its commercial availability and its frequent use in research and development projects [41].

The results of the present study showed that feeding termites with PB1000 reduced the survival rate. Both the low carbohydrate content (mainly hemicelluloses) and the presence of low molecular weight phenolics in PB1000 (such as syringaldehyde, acetosyringone) are likely to alter the physiology of the termites and jeopardize their survival. The reduction in termite survival rates caused by PB1000

was probably due to the low molecular weight phenolics as these compounds are among the mainly low molecular weight. These extractives are known to inhibit the biological activities of termites [42]. The repulsive effect of PB1000 could also explain the lower termite survival rates observed that kept the termites away from the substrate. This probably caused the termites to die by starvation. Unfortunately, there was no non-fed control, which made it impossible to draw any conclusions on this point.

However, the differences in the gut bacterial community of PB1000-fed termites compared to the controls fed on the usual birch wood-diet established that both substrates were ingested by the termites. The bacterial gut community in controls fed on birch wood was dominated by Spirochetes and Fibrobacteres. These results are consistent with studies of other *Nasutitermes* spp. [7, 25, 43]. However, the ingestion of PB1000 decreased the relative abundance of these phyla and increased Firmicutes and Bacteroidetes. Changes in the structure of the gut bacterial community were expected, as it has been well documented that dietary habits affect the

structure of the termite gut microbiota [44-46]. Of particular importance in the present study is the determination of the bacterial groups which are predominant in the microbiota of PB1000-fed termites. We used next-generation sequencing (NGS) to characterize the structure of the bacterial community. To overcome the limits of the taxonomic depth and resolution of the short sequence reads [47], we used DictDb, "a curated reference database for accurate taxonomic analysis of the bacterial gut microbiota of dictyopteran insects" [38].

Interestingly, we found that the predominant lineages were specific termite gut OTU previously reported [e.g., *Ruminococcaceae*, and *Peptococcaceae\_1*, Family\_XIII\_Incertae\_Sedis (Firmicutes) and *Porphyromonadaceae\_3*, *Porphyromonadaceae\_Gut\_Group* and *Rikenellaceae* (Bacteroidetes) [25,26]. Our findings may be valuable for the development of a bacterial inoculum for pretreatment processes in the utilization of technical grass soda lignins. The predominance of Firmicutes seems to be general in the guts of termites fed with grass-based diets [48]. Phylotypes belonging to Firmicutes have been reported to be involved in lignin degradation [22,49,50], as well as in secondary metabolite detoxification [51]. Bacteroidetes might also be involved as *Sphingobacterium* sp. T2 has recently been reported to be able to degrade industrial lignins with extracellular manganese-dependent superoxide dismutases [52]. Nevertheless, the increase of the relative abundance in Firmicutes and Bacteroidetes raises the question whether this is the result of the utilization of PB1000 as a substrate for the growth of Firmicutes and Bacteroidetes, or whether PB1000 causes the death of some phylotypes, mainly relatives of Spirochaetes and Fibrobacteres. Further studies are needed to elucidate this question.

It is worth noting that, in the present study, Py-GC/MS was found to be a suitable method for the analysis of the chemical composition of undigested and digested birch wood and PB1000. Py-GC/MS analysis of digested lignocellulosic substrates can be used directly on the guts, without any isolation or purification step. The Pyrograms of both PB1000 and birch-fed termite guts had peaks corresponding to protein-derived products, but these did not interfere with the G and S components.

In agreement with previous studies, the main compounds released by pyrolysis of PB1000 and birch wood were G and S compounds [40,53]. The release of vinylphenol from PB1000 confirmed the presence of *p*-coumaric units in this sample, as a free acid or ester. Moreover, the detection of 4-hydroxy-5,6-dihydropyran-2-one (peak 1) was consistent with the presence of some hemicellulose derivatives in PB1000, since this is created from C5 sugars [40]. It is noteworthy

that the digestion of PB1000 in termite guts induced a decrease of vanillin, syringaldehyde, and acetosyringone in the pyrograms. These results indicate that these phenolic compounds have been eliminated in the termite guts, either by the action of their microbiota or by their degradation into non-volatile.

Changes in the pyrolysis S/G ratio of the substrates after digestion support the idea that they are chemically modified in the termite digestive tract. Strikingly, although the pyrolysis S/G ratio of PB1000 was reduced by gut digestion, the pyrolysis S/G ratio of birch wood was increased. This indicates that both substrates were degraded in the guts, but by different mechanisms. That different lignin-containing substrates are degraded in different ways agrees with the literature [2]. In the case of the birchwood sample, the G and S pyrolysis products mainly originate from G and S lignin units with labile ether bonds. The reduction of the pyrolysis S/G ratio by digestion of birch wood suggests that the S lignin units with  $\beta$ -O-4 bonds were more degraded than the G lignin units with  $\beta$ -O-4 bonds.

However, as previously reported for lower termites fed with grass lignocellulose [53], the pyrolysis S/G ratio in PB1000-fed termites increased, suggesting that G lignin units might be more easily degraded than S lignin units. This preferential degradation of the G units in PB1000 might be related to the fact that most G units in grass lignins are terminal units with free phenolic groups [54], which make them more susceptible to oxidative degradation. Overall, our results suggest that a fraction of free low-molecular-weight phenolics in PB1000 was metabolized in the digestive system of *N. ephratae*.

## Conclusion

Our termite feeding experiment and Py-GC/MS analyses of gut contents was the first demonstration that the technical grass soda lignin (PB1000) can be digested by a higher wood-feeding termite, *N. ephratae*, but with a detrimental effect on the survival rate of the termites. The ingestion of PB1000 resulted in changes in the structure of the gut-bacterial community from that consistently found in *Nasutitermes* spp, in favor of Firmicutes and Bacteroidetes. The digestive system of *N. ephratae* degraded some PB1000 aromatic compounds. This was ascertained by Py-GC/MS analyses directly performed on termite guts, without any time-demanding isolation step. Overall, our results pave the way for the development of further strategies aiming at improving the survival rate of termites fed with technical lignins. They also provide insights into the bacterial groups that can be used for mimicking termite digestive strategies for the biological conversion of biorefinery wastes.



## Acknowledgements

This project received funding through the Bio-Based Industries Joint Undertaking under the European Union's Horizon 2020 research and innovation program under grant agreement No 720303. We are grateful to Dr. Richard Gosselink (FBR, Netherlands) for providing PB1000 and Dr. David Sillam-Dussès for collecting the termites. We sincerely acknowledge the financial support of the 3BCAR Institut Carnot for the acquisition of the Py-GC/MS equipment. The IJPB research unit benefits from the support of the LabEx Saclay Plant Sciences-SPS (ANR-10-LABX-552 0040-SPS).

## Funding

This project received funding through the Bio-Based Industries Joint Undertaking under the European Union's Horizon 2020 research and innovation program under grant agreement No 720303.

## Ethics Approval and Consent to Participate

Experiments were performed with termites from the collection at the French Institute for Development (IRD) – Ile de France. Termites are not considered as endangered macrofauna. The termites used in the present study were obtained with authorization.

## References

- Kamimura N, Takahashi K, Mori K, Araki T, Fujita M, et al. (2017) Bacterial catabolism of lignin-derived aromatics: New findings in a recent decade: Update on bacterial lignin catabolism. *Environ Microbiol Rep* 9(6): 679-705.
- Schutyser W, Renders T, Van den Bosch S, Koelewijn SF, Beckham GT, et al. (2018) Chemicals from lignin: an interplay of lignocellulose fractionation, depolymerisation, and upgrading. *Chem Soc Rev* 47(3): 852-908.
- Xie S, Syrenne R, Sun S, Yuan JS (2014) Exploration of Natural Biomass Utilization Systems (NBUS) for advanced biofuel--from systems biology to synthetic design. *Curr Opin Biotechnol* 27: 195-203.
- Tokuda G, Tsuboi Y, Kihara K, Saitou S, Moriya S, et al. (2014) Metabolomic profiling of <sup>13</sup>C-labelled cellulose digestion in a lower termite: insights into gut symbiont function. *Proc Biol Sci* 281(1789): 20140990.
- Hongoh Y, Deevong P, Inoue T, Moriya S, Trakulnaleamsai S, et al. (2005) Intra- and interspecific comparisons of bacterial diversity and community structure support coevolution of gut microbiota and termite host. *Appl Environ Microbiol* 71(11): 6590-6599.
- Ohkuma M, Brune A (2010) Diversity, structure, and evolution of the termite gut microbial community. In: Bignell DE, Roisin Y, Lo N, (Eds.), *Biology of Termites: A Modern Synthesis*, Springer, Dordrecht, Neth, pp: 413-438.
- Warnecke F, Luginbuhl P, Ivanova N, Ghassemian M, Richardson TH, et al. (2007) Metagenomic and functional analysis of hindgut microbiota of a wood-feeding higher termite. *Nature* 450 (7169): 560-565.
- Nakashima K, Watanabe H, Saitoh H, Tokuda G, Azuma JI (2002) Dual cellulose-digesting system of the wood-feeding termite, *Coptotermes formosanus* Shiraki. *Insect Biochem Mol Biol* 32(7): 777-784.
- Brune A, Miambi E, Breznak JA (1995) Roles of oxygen and the intestinal microflora in the metabolism of lignin-derived phenylpropanoids and other monoaromatic compounds by termites. *Appl Environ Microbiol* 61(7): 2688-2695.
- Harazono K, Yamashita N, Shinzato N, Watanabe Y, Fukatsu T, et al. (2003) Isolation and characterization of aromatics-degrading microorganisms from the gut of the lower termite *Coptotermes formosanus*. *Biosci Biotechnol Biochem* 67(4): 889-892.
- Kuhnigk T, König H (1997) Degradation of dimeric lignin model compounds by aerobic bacteria isolated from the hindgut of xylophagous termites. *J Basic Microbiol* 37(3): 205-211.
- Katsumata KS, Jin Z, Hori K, Iiyama K (2007) Structural changes in lignin of tropical woods during digestion by termite, *Cryptotermes brevis*. *J Wood Sci* 53(5): 419-426.
- Griffiths BS, Bracewell JM, Robertson GW, Bignell DE (2013) Pyrolysis-mass spectrometry confirms enrichment of lignin in the faeces of a wood-feeding termite, *Zootermopsis nevadensis* and depletion of peptides in a soil-feeder, *Cubitermes ugandensis*. *Soil Biol Biochem* 57: 957-959.
- Geib SM, Filley TR, Hatcher PG, Hoover K, Carlson JE, et al. (2008) Lignin degradation in wood-feeding insects. *Proc Natl Acad Sci U S A* 105(35): 12932-12937.
- Ke J, Laskar D, Singh D, Chen S (2013) In-situ lignocellulosic unlocking mechanism in termite for cellulose hydrolysis: critical lignin modification. *Biotechnol Biofuels* 4: 17-23.
- Ke J, Laskar DD, Chen S (2013) Varied lignin disruption mechanisms for different biomass substrates in lower termite. *Renewable Energy* 50: 1060-1064.
- Ke J, Laskar DD, Chen S (2013) Tetramethylammonium

- hydroxide (TMAH) thermochemolysis for probing in situ softwood lignin modification in each gut segment of the termite. *J Agric Food Chem* 61(6): 1299-1308.
18. Brune A, Dietrich C (2015) The Gut Microbiota of Termites: Digesting the Diversity in the Light of Ecology and Evolution. *Annu Rev Microbiol* 69: 145-166.
  19. Brune A (2014) Symbiotic digestion of lignocellulose in termite guts. *Nat Rev Microbiol* 12: 168-180.
  20. Ragauskas AJ, Beckham GT, Bidy MJ, Chandra R, Chen F, et al. (2014) Lignin valorization: improving lignin processing in the biorefinery. *Science* 344(6185): 1246843.
  21. Xu R, Zhang K, Liu P, Han H (2018) Lignin depolymerization and utilization by bacteria. *Bioresour Technol* 269: 557-566.
  22. Bugg TD, Ahmad M, Hardiman EM, Singh R (2011) The emerging role for bacteria in lignin degradation and bio-product formation. *Curr Opin Biotechnol* 22(3): 394-400.
  23. Brune A, Emerson D, Breznak JA (1995) The termite gut microflora as an oxygen sink: microelectrode determination of oxygen and pH gradients in guts of lower and higher termites. *Appl Environ Microbiol* 61(7): 2681-2687.
  24. Brown ME, Chang MC (2014) Exploring bacterial lignin degradation. *Curr Opin Chem Biol* 19: 1-7.
  25. Diouf M, Roy V, Mora P, Frechault S, Lefebvre T, et al. (2015) Profiling the succession of bacterial communities throughout the life stages of a higher termite *Nasutitermes arborum* (Termitidae, Nasutitermitinae) using 16S rRNA gene pyrosequencing. *Plos One* 10(10): e0140014.
  26. Rossmassler K, Dietrich C, Thompson C, Mikaelyan A, Nonoh JO, et al. (2015) Metagenomic analysis of the microbiota in the highly compartmented hindguts of six wood- or soil-feeding higher termites. *Microbiome* 3: 56.
  27. Akalın MK, Karagöz S (2014) Analytical pyrolysis of biomass using gas chromatography coupled to mass spectrometry. *Trends Anal Chem* 61: 11-16.
  28. Lupoi JS, Singh S, Parthasarathi R, Simmons BA, Henry RJ (2015) Recent innovations in analytical methods for the qualitative and quantitative assessment of lignin. *Renew Sust Energ Rev* 49: 871-906.
  29. Dence CW (1992) The determination of lignin. *Methods in lignin chemistry*. Springer; Berlin, Heidelberg, pp: 33-61.
  30. Sipponen MH, Lapierre C, Mechin V, Baumberger S (2013) Isolation of structurally distinct lignin-carbohydrate fractions from maize stem by sequential alkaline extractions and endoglucanase treatment. *Bioresour Technol* 133: 522-528.
  31. Lapierre C, Voxeur A, Karlen SD, Helm RF, Ralph J (2018) Evaluation of Feruloylated and p-Coumaroylated Arabinosyl Units in Grass Arabinoxylans by Acidolysis in Dioxane/Methanol. *J Agric Food Chem* 66(21): 5418-5424.
  32. Barbosa P, Berry DL, Kary CS (2015) *Insect Histology: Practical Laboratory Techniques*.
  33. Magoč T, Salzberg SL (2011) FLASH: fast length adjustment of short reads to improve genome assemblies. *Bioinformatics* 27(21): 2957-2963.
  34. Martin M (2011) Cutadapt removes adapter sequences from high-throughput sequencing reads. *EMBnet J* 17(1): 10-12.
  35. Quast C, Pruesse E, Yilmaz P, Gerken J, Schweer T, et al. (2013) The SILVA ribosomal RNA gene database project: improved data processing and web-based tools. *Nucleic Acids Res* 41: 590-D596.
  36. Rognes T, Flouri T, Nichols B, Quince C, Mahé F (2016) VSEARCH: a versatile open source tool for metagenomics. *PeerJ* 4: e2584.
  37. Mahé F, Rognes T, Quince C, de Vargas C, Dunthorn M (2014) Swarm: robust and fast clustering method for amplicon-based studies. *PeerJ* 2: e593.
  38. Mikaelyan A, Köhler T, Lampert N, Rohland J, Boga H, et al. (2015) Classifying the bacterial gut microbiota of termites and cockroaches: a curated phylogenetic reference database (DictDb). *Syst Appl Microbiol* 38 (7): 472-482.
  39. Voxeur A, Soubigou-Taconnat L, Legée F, Sakai K, Antelme S, et al. (2017) Altered lignification in mur1-1 a mutant deficient in GDP-L-fucose synthesis with reduced RG-II cross linking. *PloS One* 12(9): e0184820.
  40. Ralph J, Hatfield RD (1991) Pyrolysis-GC-MS characterization of forage materials. *J Agric Food Chem* 39(8): 1426-1437.
  41. Constant S, Lancefield CS, Weckhuysen BM, Bruijninx PC (2016) Quantification and classification of carbonyls in industrial humins and lignins by 19F NMR. *ACS Sustain Chem Eng* 5(1): 965-972.

42. Santana AL, Maranhão CA, Santos JC, Cunha FM, Conceição GM, et al. (2010) Antitermitic activity of extractives from three Brazilian hardwoods against *Nasutitermes corniger*. *Int Biodeterior Biodegradation* 64(1): 7-12.
43. He S, Ivanova N, Kirton E, Allgaier M, Bergin C, et al. (2013) Comparative metagenomic and metatranscriptomic analysis of hindgut paunch microbiota in wood- and dung-feeding higher termites. *PLoS One* 8 (4): e61126.
44. Boucias DG, Cai Y, Sun Y, Lietze VU, Sen R, et al. (2013) The hindgut lumen prokaryotic microbiota of the termite *Reticulitermes flavipes* and its responses to dietary lignocellulose composition. *Mol Ecol* 22 (7): 1836-1853.
45. Raychoudhury R, Sen R, Cai Y, Sun Y, Lietze VU, et al. (2013) Comparative metatranscriptomic signatures of wood and paper feeding in the gut of the termite *Reticulitermes flavipes* (Isoptera: Rhinotermitidae). *Insect Mol Biol* 2013; 22 (2): 155-171.
46. Su LJ, Liu YQ, Liu H, Wang Y, Li Y, et al. (2015) Linking lignocellulosic dietary patterns with gut microbial Enterotypes of *Tsaiterms ampliceps* and comparison with *Mironasutitermes shangchengensis*. *Genet Mol Res* 14 (4): 13954-13967.
47. Schloss PD, Jenior ML, Koumpouras CC, Wesrcott SL, Highlander SK, et al. (2016) Sequencing 16S rRNA gene fragments using the PacBio SMRT DNA sequencing system. *PeerJ* 4: e1869.
48. Huang XF, Bakker MG, Judd TM, Reardon KF, Vivanco JM, et al. (2013) Variations in diversity and richness of gut bacterial communities of termites (*Reticulitermes flavipes*) fed with grassy and woody plant substrates. *Microb Ecol* 65(3): 531-536.
49. Huang XF, Santhanam N, Badri DV, Hunter WJ, Manter DK, et al. (2013) Isolation and characterization of lignin-degrading bacteria from rainforest soils. *Biotechnol Bioeng* 110 (6):1616-1626.
50. Zhu D, Zhang P, Xie C, Zhang W, Sun J, et al. (2017) Biodegradation of alkaline lignin by *Bacillus ligniniphilus* L1. *Biotechnol Biofuels* 10 (1): 44.
51. Narhi LO, Fulco AJ (1986) Characterization of a catalytically self-sufficient 119,000-dalton cytochrome P-450 monooxygenase induced by barbiturates in *Bacillus megaterium*. *J Biol Chem* 261 (16): 7160-7169.
52. Rashid GM, Taylor CR, Liu Y, Zhang X, Rea D, et al. (2015) Identification of manganese superoxide dismutase from *Sphingobacterium* sp. T2 as a novel bacterial enzyme for lignin oxidation. *ACS Chem. Biol* 10 (10): 2286-2294.
53. Tarmadi D, Tobimatsu Y, Yamamura M, Miyamoto T, Miyagawa Y, et al. (2018) NMR studies on lignocellulose deconstructions in the digestive system of the lower termite *Coptotermes formosanus* Shiraki. *Sci Rep* 8 (1): 1290.
54. Lapierre C (1993) Application of new methods for the investigation of lignin structure. In Jung HG (eds.). *Forage cell wall structure and digestibility*, American Society of agronomy, Madison, Wis, pp: 133-166.

